ANTIOXIDANTS & REDOX SIGNALING
Volume 6, Number 2, 2004

Forum Original Research Communication

Endothelial Cell Proliferation Associated with Abrupt Reduction in Shear Stress Is Dependent on Reactive Oxygen Species

TATYANA MILOVANOVA,[1] YEFIM MANEVICH,[1] ALEX HADDAD,[1] SHAMPA CHATTERJEE,[1] JONNI S. MOORE,[2] and ARON B. FISHER[1]

ABSTRACT

We have shown previously that flow-adapted endothelial cells respond to cessation of flow with cell membrane depolarization and increased production of reactive oxygen species, resulting in activation of transcription factors and increased DNA synthesis. This study utilized flow cytometry to evaluate cellular proliferation with ischemia and to determine the role of reactive oxygen species and apoptosis. PKH26-labeled rat pulmonary microvascular endothelial cells were seeded in an artificial capillary system and subjected to flow at 5 dynes/cm^2 for 96 h or for 72 h followed by 24 h of simulated "ischemia." Ischemia resulted in a 2.5-fold increase in the cellular proliferation index. Cell-cycle analysis showed G0/G1 arrest and decreased S plus G2/M during flow adaptation, whereas ischemia resulted in a three-fold increase of cells in S plus G2/M phases. Apoptotic cells as detected by TUNEL and annexin V binding assays were ~5% of total cells with no differences between static, flow-adapted, and "ischemic" groups. Reactive oxygen species production during a 1-h period following onset of ischemia was confirmed by oxidation of the fluorophore, dichlorofluorescein, and was inhibited by cromakalim, a K_{ATP} channel agonist, or diphenyleneiodonium, a flavoprotein inhibitor. Cromakalim and diphenyleneiodonium also markedly inhibited cell proliferation in the flow-adapted ischemic cells, but had no effect on subconfluent cells cultured under static conditions. These results indicate reactive oxygen species-dependent endothelial cell proliferation in flow-adapted microvascular endothelial cells as a response to ischemia and indicate that this response is not a consequence of apoptosis. *Antioxid. Redox Signal.* 6, 245–258.

INTRODUCTION

THE ACUTE RESPONSE OF PULMONARY ENDOTHELIAL CELLS (EC) to the loss of shear stress associated with ischemia includes increased production of reactive oxygen species (ROS) and activation of the EC transcription factors nuclear factor-κB (NF-κB) and activator protein-1 (AP-1) (3, 4, 22, 26). We have proposed that EC "sensing" of abrupt cessation of shear stress (the mechanotransduction hypothesis) is the initiating factor for the biochemical events that lead to activation of endothelial NADPH oxidase and ROS generation (12, 13). Ischemia also was associated with increased EC division (26). After 24 h of ischemia, flow-adapted bovine pulmonary artery endothelial cells (BPAEC) demonstrated twice as much [^{3}H]-thymidine incorporation as control cells, as well as cellular G0/G1 arrest and concomitant increase in the number of cells in S phase by cell-cycle analysis (26). The physiological significance of increased cell division associated with loss of shear stress could be considered as an attempt to generate new capillaries to restore the impeded blood flow.

[1]Institute For Environmental Medicine and [2]Abramson Cancer Center Flow Cytometry and Cell Sorting Shared Resource and Department of Pathology and Laboratory Medicine, University of Pennsylvania Medical Center, Philadelphia, PA 19104–6068.

It has been suggested that shear stress is an important physiological regulator of EC function and may play a key antiatherogenic role by maintaining EC stability through blocking of cell-cycle progression that is associated with their proliferation (1). Further, apoptosis of EC can be regulated by shear stress. High laminar shear stress inhibited apoptosis of EC *in vitro* (7, 10, 15). *In vivo,* apoptosis occurs preferentially downstream of atherosclerotic plaques, where eddies and separation of blood stream from the vessel wall result in low mean shear stress (25).

The goal of the present study was to investigate further microvascular cell proliferation with an *in vitro* model of lung ischemia. Ischemia was produced by interruption of medium flow while maintaining oxygenation of EC that had been preadapted to shear stress in culture. Whereas the previous studies evaluated BPAEC (26), this study utilized rat pulmonary microvascular endothelial cells (RPMVEC) to provide correlation with our *in vivo* studies of rat lungs. We developed criteria for RPMVEC proliferation *in vitro* and evaluated the roles for ROS and apoptosis as signals for cellular proliferation.

MATERIALS AND METHODS

Cells and culture media

RPMVEC were obtained originally from Dr. T. Stevens (University of South Alabama) (24) and maintained in our laboratory as described previously (9). Cells were propagated in Dulbecco's modified Eagle medium (DMEM) supplemented with 10% fetal bovine serum (FBS), nonessential amino acids, and penicillin/streptomycin. Cells were maintained under static culture conditions for several passages before they were subjected to flow. Cells between the passages 5 and 20 were used for experiments. The endothelial phenotype of the preparation was routinely confirmed by evaluating cellular uptake of DiI-acetylated low-density lipoprotein (DiIAcLDL) and the presence of platelet EC adhesion molecule (PECAM-1 or CD31).

Cell culture in an artificial capillary system

RPMVEC were cultured under flow of culture medium (DMEM) using commercially available artificial capillary technology (Cell Max, FiberCell Systems Inc., Frederick, MD, U.S.A.) as described previously (9, 26, 27). In brief, each Cell Max system comprises a central pump station capable of accommodating four flow paths with cartridges. Each cartridge consisted of 230 semipermeable polypropylene hollow fibers ("artificial capillaries") mounted in a hard polycarbonate casing, with ports allowing perfusion via either the luminal or abluminal compartment.

Prior to cell seeding, the inner lumen of the "capillary" fibers was coated with ProNectin F (Sanyo Chem Industries, Kyoto, Japan). Freshly harvested cells from two confluent T 75 flasks of RPMVEC (12–16 $\times$ 10^6 cells) were seeded per cartridge. To allow attachment of RPMVEC to the capillary fibers, the perfusing medium was routed to the abluminal side for a 24-h period. The perfusion circuit then was rerouted to the luminal side so that cells were subjected to shear. Cells were cultured under steady laminar flow, generally for 48–72 h using a flow rate sufficient to generate 5 dynes/cm^2 shear stress. Shear rate was calculated from specifications supplied by the manufacturer of the Cell Max modules. The cartridge environment was maintained at 37°C and 5% CO_2 in a humidified incubator.

Simulated ischemia

"Ischemia" was simulated by rerouting the flow from the luminal to the abluminal compartment. This protocol eliminated cellular shear stress, but allowed continued oxygenation. We showed previously by analysis using an oxygen electrode of medium samples obtained from the cartridge lumen that Po_2 during abluminal flow (ischemia) is similar to control (26). For most experiments, control cells were grown under flow or static conditions for 96 h, whereas experimental cells were grown under flow for 72 h followed by 24 h of stop flow (ischemia). At the end of the control (static or flow) or experimental (ischemia) period, cells were removed from the cartridges with 0.25% trypsin for 5 min, centrifuged at 1,400 *g* at 4°C for 5 min, and then analyzed by flow cytometry or confocal microscopy.

Confocal microscopy

Confocal microscopy (Radiance 2000, Bio-Rad, Hercules, CA, U.S.A.) was used to image cultured cells trypsinized from cartridges. Cells were centrifuged at 1,400 *g* for 5 min and then placed on a glass slide for observation at 600$\times$ magnification. The number of cells in the microscopic field was determined using ImagePro software (Media Cybernetics, Silver Spring, MD, U.S.A.).

Flow cytometry

Flow cytometry was performed with a four-color, dual laser FACSCalibur (Becton–Dickinson, San Jose, CA, U.S.A.). The assay utilized monoclonal antibody to CD31 (BD-Pharmingen, Palo Alto, CA, U.S.A.) conjugated with streptavidin fluorescein isothiocyanate (FITC) (Caltag, Burlingame, CA, U.S.A.) or streptavidin APC (BD-Pharmingen) to identify EC. CD31-FITC was measured in the FL-1 channel, PKH26 and propidium iodide in the FL-2 channel, and TO-PRO-3 and CD31APC in the FL-4 channel. Compensation for PKH26 was concentration-dependent and was determined empirically. Quantitative analysis of proliferation was performed using CellQuest™ acquisition/analysis software (Becton–Dickinson) and the Proliferation Wizard™ module in ModFit LT™ Macintosh software (Verity Software House, Topsham, ME, U.S.A.) by collecting 5 $\times$ 10^4 events. CellQuest and FlowJo (Tree Star, Ashland, OR, U.S.A.) programs were used for analysis of surface or intracellular staining.

Cell proliferation

Proliferation of RPMVEC was studied by labeling with PKH26, a lipid membrane dye, and analyzed by flow cytometry. For labeling, cells were washed once in RPMI 1640 medium containing 8% FBS, followed by two serum-free washes. The cell pellet was then taken up in Dilutant C (Sigma, St. Louis, MO, U.S.A.) to achieve a suspension of 5 $\times$ 10^6 cells/ml. The dilutant from the PKH26-GL Cell Linker Kit is designed to promote dispersal of the lipophilic dye. This cell suspension was then added to an equal volume of PKH26 dye stock (either 2 or 4 $\times$ 10^{-6} *M*); these concentrations were previously estab-

lished to stain cells homogeneously with little loss of viability and at appropriate levels for spectral compensation. Cells were incubated for 3 min at room temperature, diluted 1:1 with heat-inactivated FBS, centrifuged to a pellet three times, washed with RPMI medium with serum and then with AIM V (Gibco-BRL, Gaitherburg, MD, U.S.A.) supplemented with 1 m*M* sodium pyruvate, 2 m*M* L-glutamate, nonessential amino acids, 55 μ*M* 2-mercaptoethanol, 25 m*M* HEPES, and then counted with either a hemocytometer or Coulter counter (model Z2). After labeling, cells were cultured under static or flow conditions and used for ischemia experiments.

For analysis of cell proliferation by flow cytometry, all events were plotted in a CD31-FITC versus side scatter plot (SSC-H), and a gate was set around the CD31-positive cells indicating the EC population (R1 in Fig. 1a). The gated data were plotted in a contour plot FL-4 on the ordinate and SSC-H on the abscissa to identify a viable (TO-PRO-3 negative) population (R2 in Fig. 1b). A gate was set for the TO-PRO-3-negative population and FL-1 was plotted against FL-2 to identify the population doubly positive (for CD31-FITC and PKH26; R3 in Fig. 1c). Proliferation was calculated from the R3 gate using the ModFit program based on the fluorescence content of cell populations as illustrated in Fig. 1d and from the CellQuest program based on the sum of R1, R2, and R3. The ModFit software deconvolves the fluorescence intensity histograms to calculate the proportion of cells in each of these Gaussian distributions (14, 23). The proliferation index is the ratio of the sum of the proliferated cells (generation G2, etc.) to the unproliferated parental generation. The percentage of cells that proliferated was calculated from total cells minus the percentage of cells remaining in the parental generation.

Cell cycle analysis

RPMVEC (1×10^6) were pelleted and fixed with 70% ice-cold ethanol, followed by the incubation with RNase (100 μg/ml) and propidium iodide (4 μg/ml) in phosphate-buffered saline (PBS). RPMVEC that were labeled with PKH26 were permeabilized with 2% paraformaldehyde for 20 min on ice, followed by 0.1% Triton X-100 for 5 min at room temperature. Cell cycle phases of the diploid population were analyzed by flow cytometry using the ModFit program based on cellular DNA content (11). The tetraploid and aneuploid populations were defined by their abnormal content of DNA based on analysis of histograms. Tetraploid and aneuploid populations of cells were excluded from the cell-cycle analysis.

Detection of proliferating cell nuclear antigen by immunofluorescence

An antibody against PCNA was used to identify cells undergoing DNA synthesis (18). Cells after trypsinization from the cartridges were fixed in 100% methanol for 1 h on ice, washed in PBS, incubated in 0.1% Tween 20 in PBS for 30 min at room temperature, and then incubated in blocking solution (2% dry milk, 0.1% Tween 20 in PBS) for 30 min. For antigen detection, cells were incubated with mouse anti-PCNA (BD-Pharmingen; 1:200) for 1 h, followed by FITC goat anti-mouse IgG, diluted 1:200. Cells were centrifuged at 1,400 *g* for 5 min, then mounted on glass slides with AquaPolyMount, and examined using confocal scanning laser microscopy. At least six fields were examined and photographed with the confocal microscope.

Annexin V staining

Apoptosis was assessed by measuring FITC-annexin V staining. Experimental RPMVEC were trypsinized, harvested, and washed once with serum-containing medium before incubation with annexin V. The cells were suspended at 1×10^6 cells/ml, rinsed with 10 m*M* HEPES, pH 7.4, 140 m*M* NaCl, 2.5 m*M* $CaCl_2$, and resuspended in 200 μl of this binding buffer. Aliquots (100 μl) of the cell solution were then stained with FITC-annexin V (BD-Pharmingen) and propidium iodide (50 μg/ml), incubated at room temperature for 5–15 min in the dark, and analyzed by flow cytometry.

Terminal dUTP nucleotide end labeling (TUNEL) assay by flow cytometry

For TUNEL assay, RPMVEC following removal from the cartridges were treated using an APO-DIRECT kit (BD-Pharmingen) according to the manufacturer's recommendations. In brief, 1×10^6 RPMVEC were fixed with 4% (wt/vol) electromicroscopic grade paraformaldehyde in PBS on ice for 60 min. After centrifugation, cells were resuspended in ice-cold 70% (vol/vol) ethanol and incubated for 1 h at −20°C for permeabilization. Cells were washed twice with washing buffer (PBS with 0.2% bovine serum albumin), and the cell pellet then was incubated at 37°C for 60 min with staining solution [10 μl of reaction buffer, 1 μl of TdT enzyme, 8 μl of 2′-deoxyuridine 5′-triphosphate (FITC-dUTP or Cy5 dUTP), and 31 μl of distilled water]. After two washes with rinse buffer, the cell pellet was resuspended in a propidium iodide/RNase A solution, incubated for 60 min in the dark, and analyzed by flow cytometry. Prefixed apoptotic cells included in the kit and also RPMVEC treated for 24 h with 1.2 mg/ml tumor necrosis factor α (TNFα; BD Biosciences) were used as positive controls. Cells incubated with the staining solution minus TdT enzyme served as a negative control.

Oxidant generation

Oxidant generation was assessed by pre-loading cells with 10 μ*M* 2′,7′-dichlorodihydrofluorescein (H_2DCF) diacetate (Kodak, Rochester, NY, U.S.A.) and measuring its conversion to fluorescent dichlorofluorescein (DCF). Cells were flow-adapted for 72 h at 5 dynes/cm^2, and H_2DCF diacetate was added to the perfusate during the final 1 h.

Cells then were subjected to either 1 h of additional continuous flow (control) or 1 h of simulated ischemia. The perfusate during the loading and experimental periods was changed from DMEM to Krebs–Ringer bicarbonate solution, pH 7.4. In some experiments, 10 μ*M* diphenyleneiodonium chloride (DPI; ICN Biomedicals, Cleveland, OH, U.S.A.) or 30 μ*M* cromakalim (Sigma) was added to the incubation medium during the dye loading and experimental periods.

Statistics

Results are expressed as the means ± SE for three or more independent experiments. Significance was determined by ANOVA or *t* test as appropriate using SigmaStat (Jandel Sci-

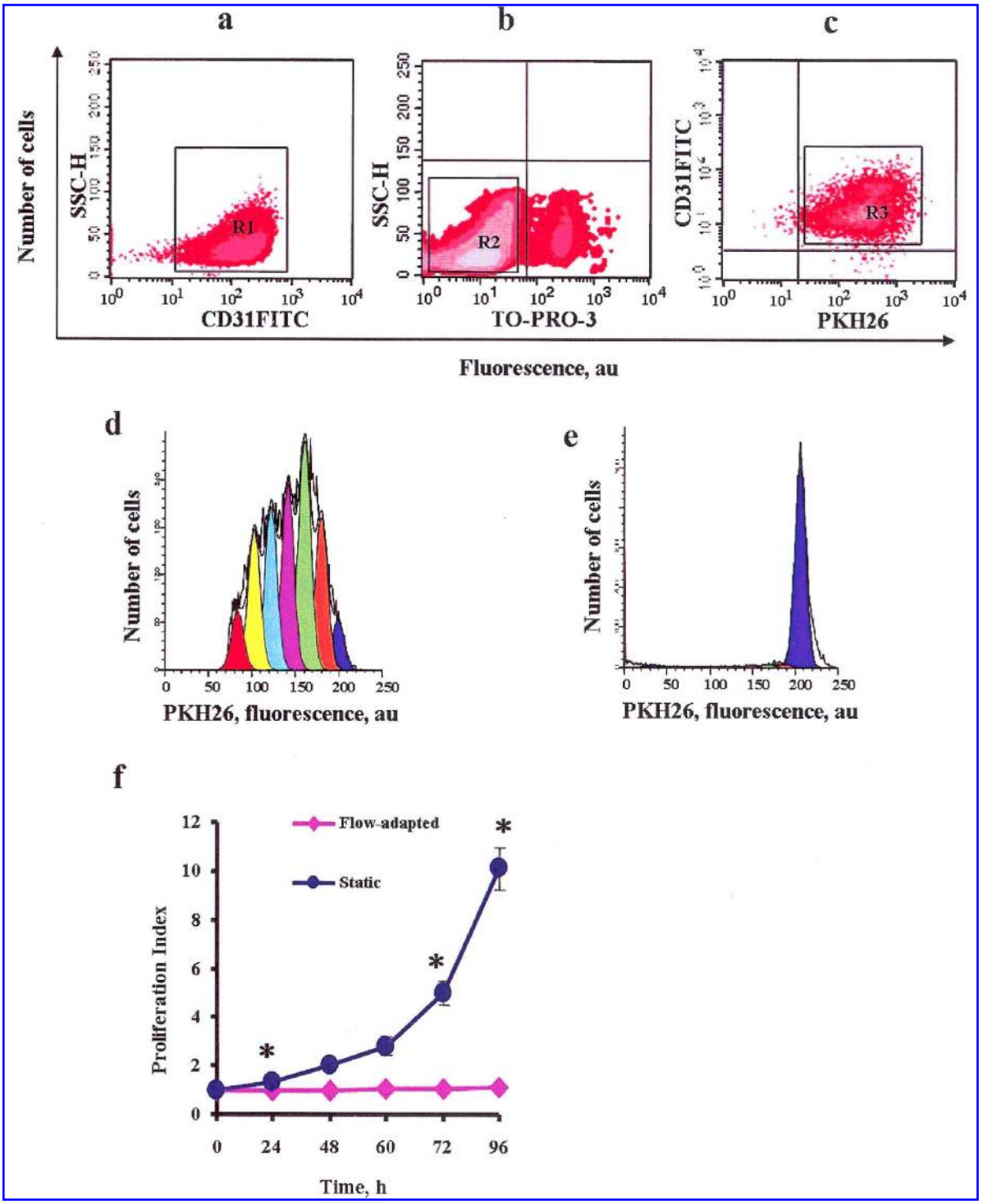

FIG. 1. Method for analysis of cell proliferation with the fluorescence-activated cell sorter (FACS) using the fluorophores CD31-FITC/PKH26/TO-PRO-3. (**a**) Cells were sorted by a side scatter plot (SSC-H) versus CD31-FITC. CD31-FITC-positive cells (R1) represent the EC population. (**b**) TO-PRO-3 was used to discriminate between dead and live cells. The TO-PRO-3-negative cells (R2) represent the live population. (**c**) The doubly positive CD31-FITC/PKH26 population indicating labeled EC (R3) was analyzed for proliferation. (**d**) Proliferation of RPMVEC after 96 h in static culture (abluminal flow). Deconvolution of the histogram distributions into generations (indicated by different shades of gray) was performed by ModFit software as described in the text. The proliferation index in this example is 10.2. (**e**) Proliferation of RPMVEC after 96 h of flow at a shear stress of 5 dynes/cm^2. The proliferation index in this example is 1.0. (**f**) Proliferation index of CD31-FITC/PKH26-positive cells after incubation for 24–96 h under static or flow-adapted conditions. The values represent the means ± SE for $n = 4$. *$p < 0.05$ compared with the preceding time point value on the curve. au, arbitrary units.

entific, San Jose, CA, U.S.A.), and the level of statistical significance was defined as $p < 0.05$.

RESULTS

Proliferation of subconfluent RPMVEC

RPMVEC were seeded at a subconfluent density (1×10^6 cells per cartridge) and evaluated after flow adaptation in cartridges for 48–96 h under 5 dynes/cm^2 shear stress or following a similar period of static culture. The nominal times described in this report do not include the initial 24-h attachment period used for all experiments. A typical experiment is shown in Fig. 1. Cells were sorted for CD31 positivity (Fig. 1a) representing >95% of cells, TO-PRO-3 negativity (Fig. 1b) representing >90% of cells, and PKH26 positivity (Fig. 1c.) representing >95% of cells. The proliferation index of cells at day 0 was set to 1.0. The fluorescence distribution of RPMVEC cultured in cartridges under abluminal flow (*i.e.,* static culture) for the same period of time showed multiple peaks indicating cell division (Fig. 1d). On the other hand, the fluorescence distribution for cells cultured for 96 h under flow showed a single peak (Fig. 1e). The proliferation index in the static cells ranged from 1.0 (day 0) to 10.2 (day 5) (Fig. 1f). The proliferation index of RPMVEC subjected to flow was similar to day 0 for all time periods up to 96 h (proliferation index 1.0 ± 0.02) (Fig. 1f). Thus, cells cultured under static conditions (abluminal flow) showed rapid proliferation, whereas cells subjected to a shear stress of 5 dynes/cm^2 (luminal flow) did not proliferate.

Conditions for cellular confluence

The cells cultured in the cartridges were evaluated for confluence because that could influence the subsequent proliferative response to ischemia. Cells were seeded at either $4–5 \times 10^6$ or $12–16 \times 10^6$ per cartridge and cultured for 12 or 24 h under static conditions. With seeding at the lower density, cell-cycle analysis of RPMVEC trypsinized from the cartridges at 24 h showed a significant number of cells in S and G2/M phases (Fig. 2a and d). At the higher density, cells trypsinized at 12 h showed a significant percentage in S phase (Fig. 2b and d), whereas there was cell-cycle arrest in G1/G0 after 24 h (Fig. 2c and d).

Cells were also evaluated for confluence by PCNA immunofluorescence. Cells that were seeded at $4–5 \times 10^6$ per cartridge and cultured for 24 h showed positive PCNA fluorescence, indicating active DNA synthesis (Fig. 2e). Cells seeded at $12–16 \times 10^6$ and cultured for 24 h were negative for PCNA staining (Fig. 2g), whereas cells seeded at this density and cultured for only 12 h showed intermediate fluorescence (Fig. 2f). These results for PCNA staining and cell-cycle analysis show good correlation and indicate cellular confluence at 24 h following seeding with $12–16 \times 10^6$ cells per cartridge.

Cellular proliferation with simulated ischemia

The proliferation assay was used to determine whether RPMVEC proliferate under simulated ischemia following a period of flow adaptation. Cells were seeded in the cartridges at the density that promoted confluence. Cells were adapted to flow for periods of 24–72 h and then subjected to 24 h of ischemia. Significant proliferation was observed by ischemic cells that had been flow-adapted and varied as a function of duration of flow adaptation (Fig. 3a). The proliferation index doubled in RPMVEC that had been flow-adapted for 60–72 h, with a lesser increase in cells after 48 h of flow adaptation (Fig. 3b). Approximately 80% of the cells in the 72-h flow-adapted group subjected to 24 h of ischemia had proliferated (Fig. 3c).

Cells were evaluated for the effect of ischemia on their distribution in the cell cycle. Control cells that had been flow-adapted for 72 h demonstrated cell-cycle arrest in the G1/G0 phase (Fig. 4a). By contrast, ischemia led to a decreased number of cells in G1/G0 phases and a three-fold increase in the number of cells in S plus G2/M phases (Fig. 4b), changes that were statistically significant (Fig. 4c). Thus, ischemic cells showed entry into the cell cycle and cellular proliferation. This analysis was based on the diploid population only. The incidence of tetraploid and aneuploid cells was ~1% for static and flow-adapted cells and was 15% in the ischemic population.

The yield of cells following trypsinization from the cartridges was determined by counting with the Coulter counter. The cartridges were seeded at a density ($12–16 \times 10^6$ cells per cartridge) that promoted confluence. Cell recovery per cartridge at the end of experiments was 19.9 (± 0.56) $\times 10^6$ for cells cultured under static conditions for 96 h, 14.3 (± 2.9) $\times 10^6$ for cells cultured under flow for 96 h, and 17.6 (± 1.5) $\times 10^6$ for cells that were flow-adapted for 72 h, followed by 24 h of ischemia ($n = 4–5$; $p > 0.05$). Analysis of the recirculating medium at the end of the experiments showed that fewer than 4% of cells were unattached, with no significant difference between the three conditions. The flush solution prior to trypsinization yielded 4.3% of the statically cultured cells, 26.4% of the flow-adapted cells, and 10.4% of the flow-adapted/ischemic cells. These results indicate that cells cultured under shear stress might be more loosely attached to the underlying substratum. The remainder of the cells were obtained by the trypsinization step. A subsequent trypsinization with twice the concentration of trypsin (0.5%) yielded no further cells. The number of TUNEL- and TO-PRO-3-positive cells was similar for cells recovered in the flush solution or following trypsinization. Although the differences in yield among the three groups are not statistically different, the pattern is compatible with flow-mediated inhibition of cell proliferation and subsequent proliferation associated with ischemia.

Apoptosis in RPMVEC

We investigated the possibility that apoptosis was the stimulus for cellular proliferation with ischemia. Annexin V binding and TUNEL assay were used to detect apoptosis in RPMVEC following their removal from the cartridges. Annexin V binding was evaluated by flow cytometry. Cells cultured under flow conditions for 96 h showed a single peak with a negligible high fluorescence population, indicating that there was essentially no population of cells that bound annexin V (Fig. 5a). Cells that were ischemic for the final 24 h of culture showed a pattern for annexin V binding on flow cytometry that was similar to that shown by cells cultured under flow (Fig. 5b). A positive control demonstrates a population with ~50% of cells that bound annexin V following 24 h incubation with TNFα (Fig. 5c).

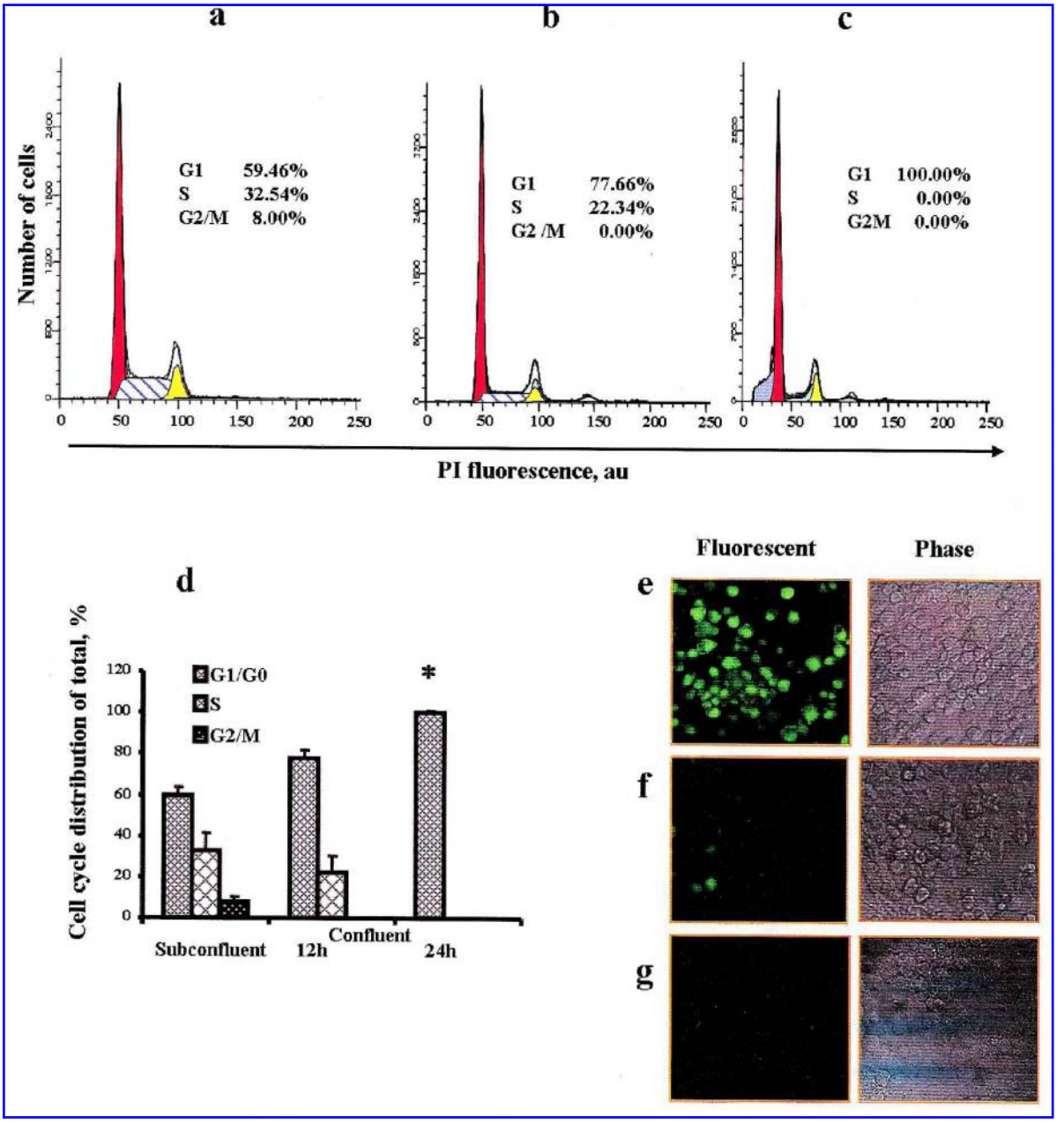

FIG. 2. Analysis of conditions for RPMVEC confluence. Cells were cultured in the artificial capillaries under static conditions and then harvested by trypsinization. (**a–d**) FACS analysis of the distribution of diploid cells in G1/G0, S, or G2/M expressed as a percentage of total cells. Quantitation of peaks considered only the diploid population. The peaks are: G1 (dark gray), S (striped), G2/M (white), and aneuploid cells (light gray). (**a**) Initial seeding 4×10^6 cells; cultured for 24 h (subconfluent). (**b**) Initial seeding 12×10^6 cells; cultured for 12 h (confluent 12 h). (**c**) Initial seeding 12×10^6 cells; cultured for 24 h (confluent 24 h). (**d**) Cell-cycle analysis for $n = 3$ for each condition. Values are means ± SE. *$p < 0.05$ vs. subconfluent. (**e–g**) Fluorescence and corresponding phase-contrast images for cells stained with antibody to PCNA. (**e**) Subconfluent cells. (**f**) Confluent 12-h cells. (**g**) Confluent 24-h cells. au, arbitrary units.

Apoptosis also was evaluated by TUNEL assay. Cell fluorescence in the absence (Fig. 6a, left panel) and presence (Fig. 6a, right panel) of the enzyme TdT confirms the validity of the assay. Approximately 5% of cells cultured under static conditions were TUNEL-positive (Fig. 6a and b). There was no significant change in the percent apoptosis for cells that were flow-adapted for 96 h (Fig. 6b and c) or flow-adapted for 72 h, followed by 24 h of ischemia (Fig. 6b and d). There was approximate doubling in the percent apoptosis of cells from passage 19 compared with passage 5, but there were no significant differences between static, flow-adapted, and ischemic cells from the same passage (data not shown). As a control, a pop-

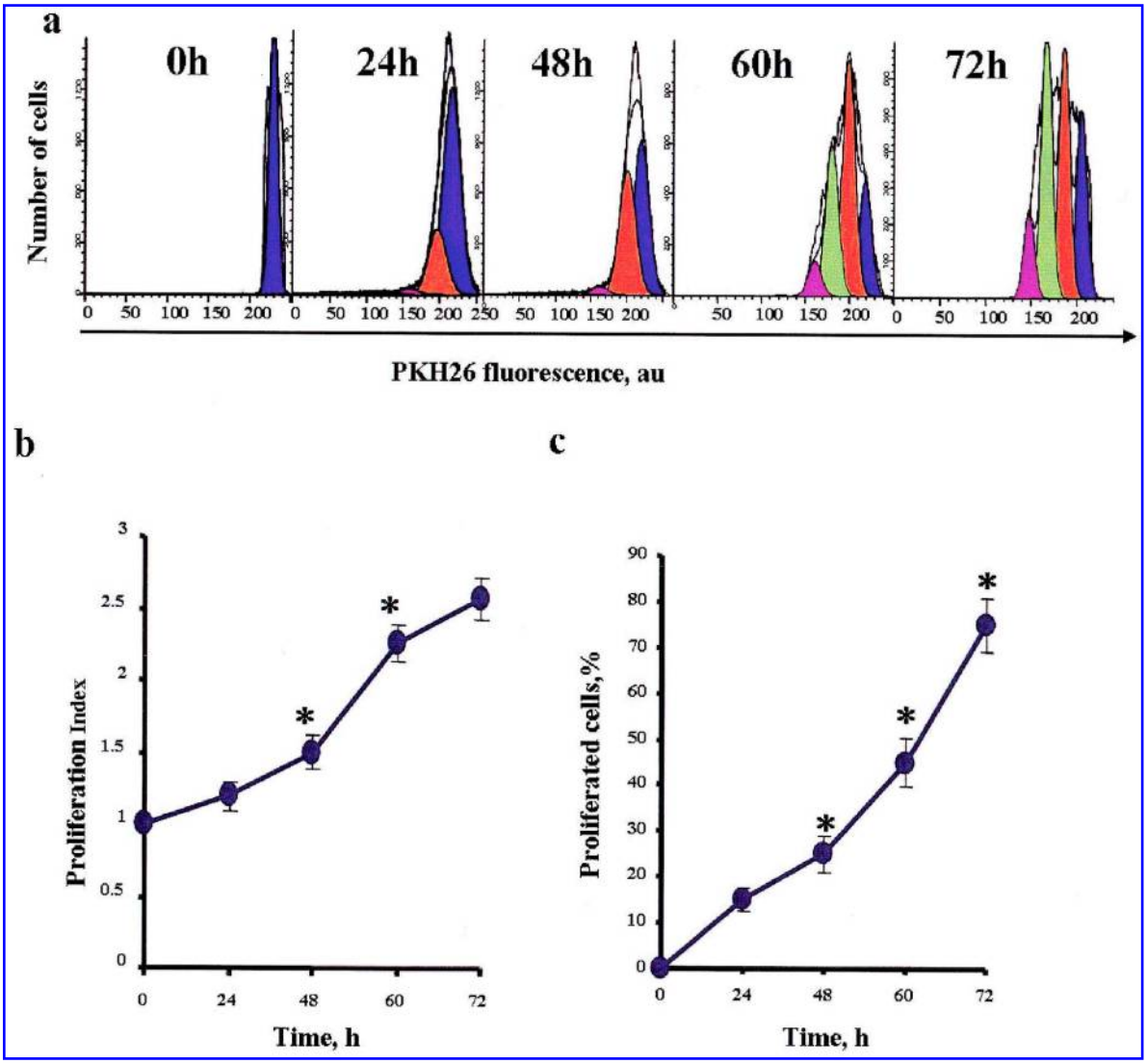

FIG. 3. Effect of duration of flow adaptation on subsequent proliferation of PKH26-labeled RPMVEC with ischemia. PKH26-labeled PMVEC were cultured for varying duration (0–72 h) under a shear stress of 5 dynes/cm^2 and then subjected to 24 h of ischemia. Cells were removed from the cartridges, and CD31-FITC-positive cells were analyzed by FACS for PKH26 fluorescence. (**a**) Deconvolution of the histograms into generations for the indicated duration of flow adaptation prior to ischemia was performed by ModFit Software. (**b**) Proliferation index and (**c**) % proliferated cells derived from generational histograms are plotted as a function of time of adaptation to 5 dynes/cm^2 shear stress. Values are means ± SE for $n = 5$. *$p < 0.05$ compared with the preceding time point value on the curve. au, arbitrary units.

ulation of ~25% TUNEL-positive cells was demonstrated following 24 h of incubation with TNFα (Fig. 6e).

Role of ROS in proliferation of RPMVEC with ischemia

DCF was used to evaluate cellular generation of ROS. Cells were cultured under static conditions or flow for 72 h, followed by 1 h of ischemia. Oxidation of H_2DCF as determined by confocal microscopy was at a relatively low level in flow-adapted cells (Fig. 7a), but markedly increased with ischemia (Fig. 7b). Increased fluorescence was observed in nearly all of the cells that were examined. ROS generation with ischemia was markedly inhibited by the presence of the flavoprotein inhibitor, DPI (Fig. 7c), or the K_{ATP} channel agonist, cromakalim (Fig. 7d). DPI presumably inhibits the NADPH oxidase by binding to its flavoprotein component, whereas cromakalim prevents the ischemia-mediated membrane depolarization that results in NADPH oxidase activation (9, 22). The increased DCF fluorescence with ischemia (Fig. 7e) and its inhibition by DPI (Fig. 7f) and by cromakalim (Fig. 7g) were confirmed by flow cytometry.

Treatment with cromakalim (30 μ*M*) or DPI (10 μ*M*) was used to evaluate the role of ROS in RPMVEC proliferation with ischemia. These agents were added to the medium during the final 1 h of the 72-h flow adaptation period prior to the start

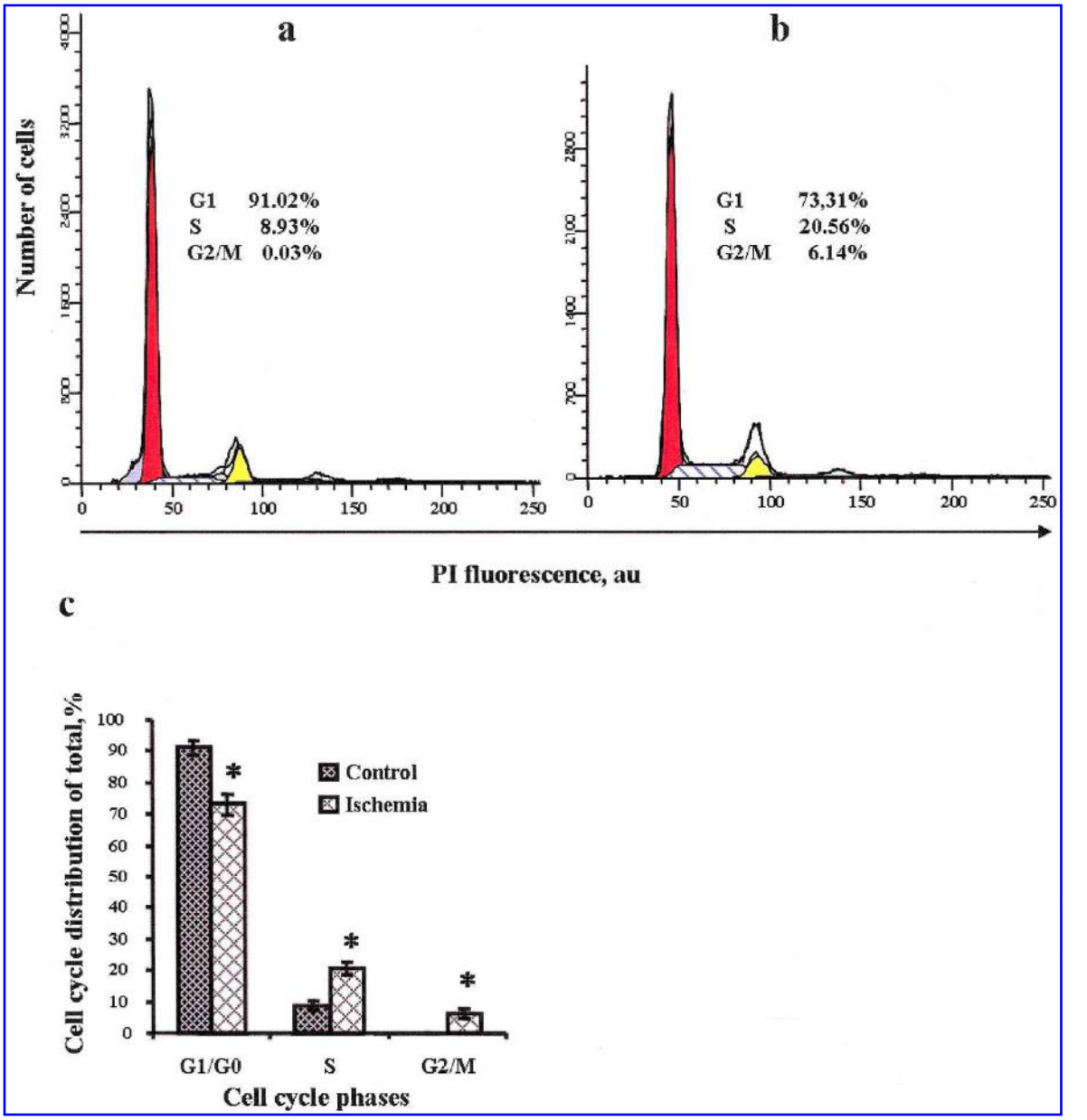

FIG. 4. Effect of flow adaptation and subsequent ischemia on cell-cycle progression. Cells were cultured under flow (5 dynes/cm^2) for 94 h (**a**) or 72 h followed by 24 h of ischemia (**b**). Histograms of DNA content of RPMVEC during the cell cycle were generated by FACS analysis following removal of cells from the cartridge. The distribution of diploid cells in G1/G0, S, and G2/M is expressed as a percentage of total cells. (**c**) Means ± SE for $n = 3$. *$p < 0.05$ for ischemia vs. corresponding control (continuous flow) value. au, arbitrary units.

of the 24-h ischemia or 24-h continued flow period. Ischemia for 24 h resulted in the expected proliferative response (proliferation index 2.4; Fig. 8a). This proliferative response was markedly inhibited by the presence of DPI (proliferation index 1.2; Fig. 8b) or cromakalim (proliferation index 1.2; Fig. 8c). Inhibition of the response by both agents was statistically significant ($p < 0.05$) (Fig. 8g). Inhibition of proliferation by two mechanistically unrelated inhibitors of ROS generation indicates a major role for ROS in the proliferative response to ischemia.

The effect of cromakalim and DPI on proliferation of cells grown under static conditions was studied with subconfluent cultures under abluminal flow in the artificial capillary cartridges. Subconfluent culture showed proliferation in the absence of inhibitors (Fig. 8d). The addition of DPI or cromakalim had no significant effect on proliferation of static subconflu-

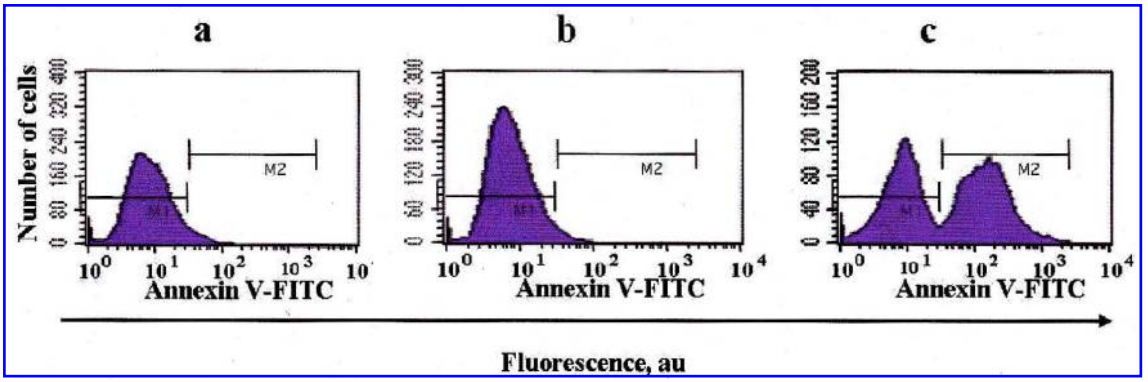

FIG. 5. Annexin V binding to RPMVEC. The cellular distribution of annexin V FITC binding determined by FACS. The fluorescence in arbitrary units (au) is indicated on a logarithmic scale. The presence of annexin V-labeled cells is demonstrated by a subpopulation of cells with increased fluorescence intensity in the M2 gate. (**a**) RPMVEC were subjected to 24 h of ischemia following 72 h of flow adaptation. (**b**) RPMVEC were maintained for 24 h in static culture (negative control). (**c**) RPMVEC were incubated with 1.2 mg/ml TNFα during 24 h of static culture (positive control).

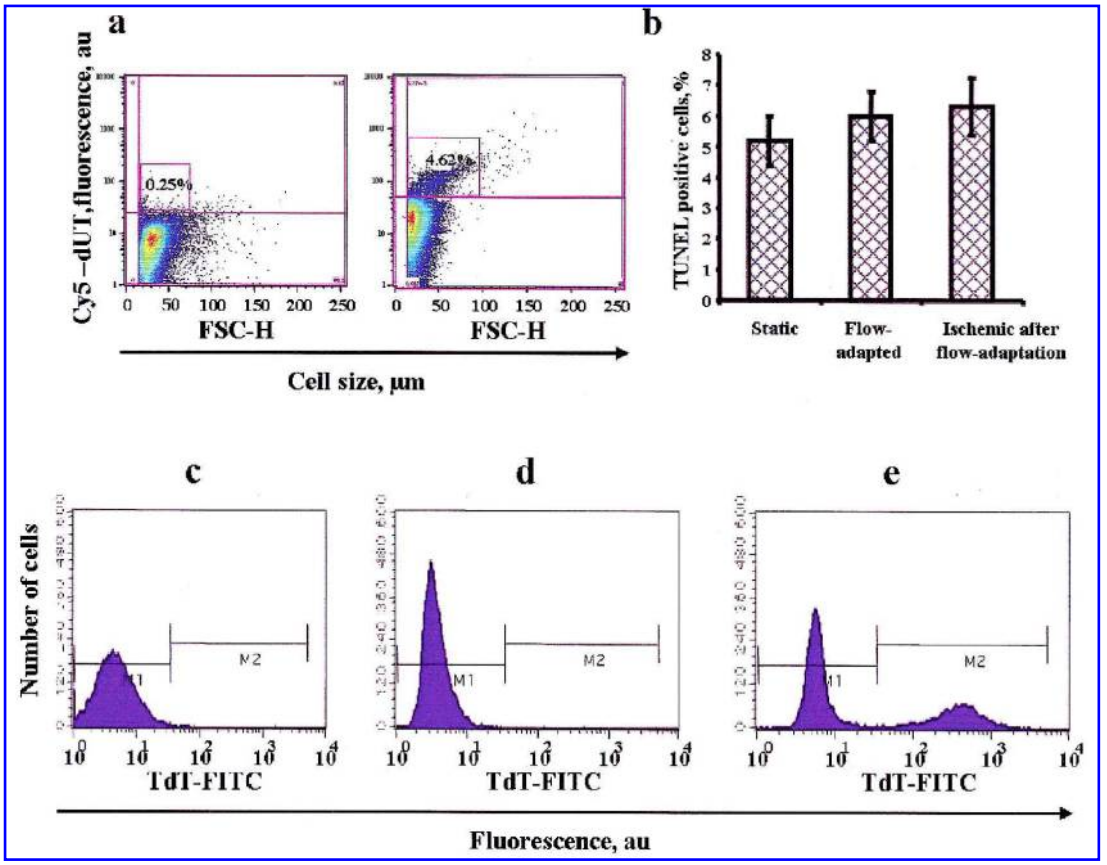

FIG. 6. TUNEL analysis of RPMVEC. The cellular distribution of Cy5dUTP- or FITC dUTP-labeled RPMVEC was determined by FACS using experimental conditions parallel to those shown in Fig. 5. (**a**) Analytical control showing cell distribution in the absence (**left panel**) and presence (**right panel**) of the TdT enzyme. The numbers above the box indicate the % positive cells. (**b**) Percentage of TUNEL-positive cells for RPMVEC cultured under static conditions, flow-adapted for 96 h, or flow-adapted for 72 h followed by 24 h of ischemia. The results are means ± SE for $n = 4$. The difference between conditions is not statistically significant ($p > 0.05$). (**c–e**) Examples of individual experiments for TUNEL. The fluorescence is indicated in arbitrary units (au) on a logarithmic scale. The presence of TUNEL-positive cells is demonstrated by a subpopulation of cells with increased fluorescence intensity in the M2 gate. (**c**) RPMVEC were subjected to 24 h of ischemia following 72 h of flow adaptation. (**d**) RPMVEC were maintained for 24 h in static culture (negative control). (**e**) RPMVEC were incubated with 1.2 mg/ml TNFα during 24 h of static culture (positive control).

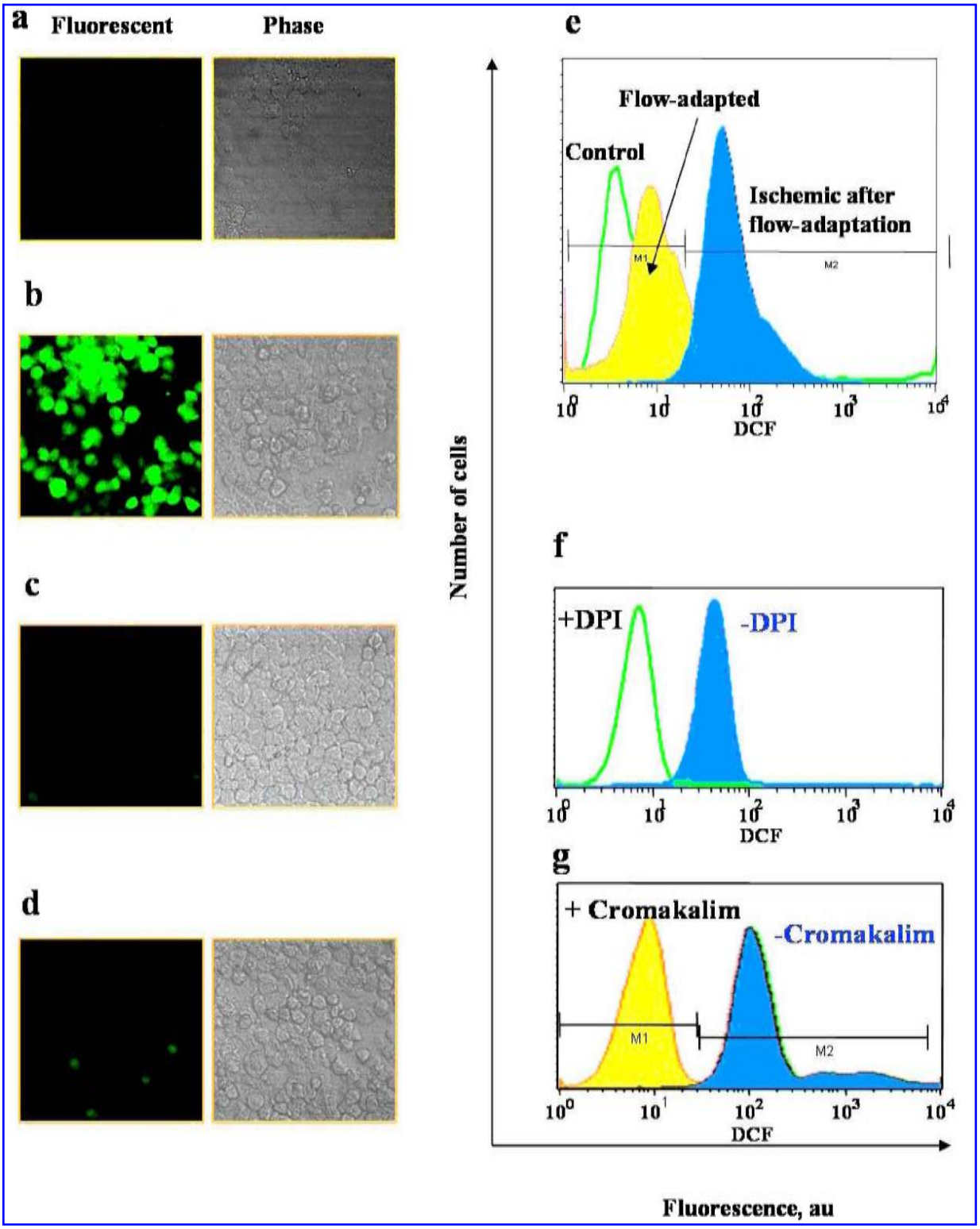

FIG. 7. ROS generation by RPMVEC as indicated by the distribution of DCF fluorescence. Cells cultured in artificial capillaries were preincubated with H_2DCF diacetate for 30 min, incubated for an additional 1 h, and then trypsinized from the cartridges. Inhibitors were present during the 30-min preincubation plus 1-h experimental periods. (**a–d**) Cells were evaluated by fluorescence and phase-contrast microscopy using the confocal microscope. (**a**) 72 h of flow-adapted RPMVEC followed by 1 h of additional flow. (**b**) 72 h of flow-adapted RPMVEC followed by 1 h of ischemia. (**c**) 72 h of flow-adapted RPMVEC followed by 1 h of ischemia in the presence of 10 μ*M* DPI. (**d**) 72 h of flow-adapted RPMVEC followed by 1 h of ischemia in the presence of 30 μ*M* cromakalim. (**e–g**) FACS analysis of DCF-labeled cells. (**e**) Cell distribution for static cells, flow-adapted cells (73 h of flow), and ischemic cells (72 h of flow plus 1 h of ischemia). (**f**) Ischemic cells (72 h of flow followed by 1 h of ischemia) in the absence and presence of 10 μ*M* DPI. (**g**) Ischemic cells (72 h of flow followed by 1 h of ischemia) in the absence and presence of 30 μ*M* cromakalim. au, arbitrary units.

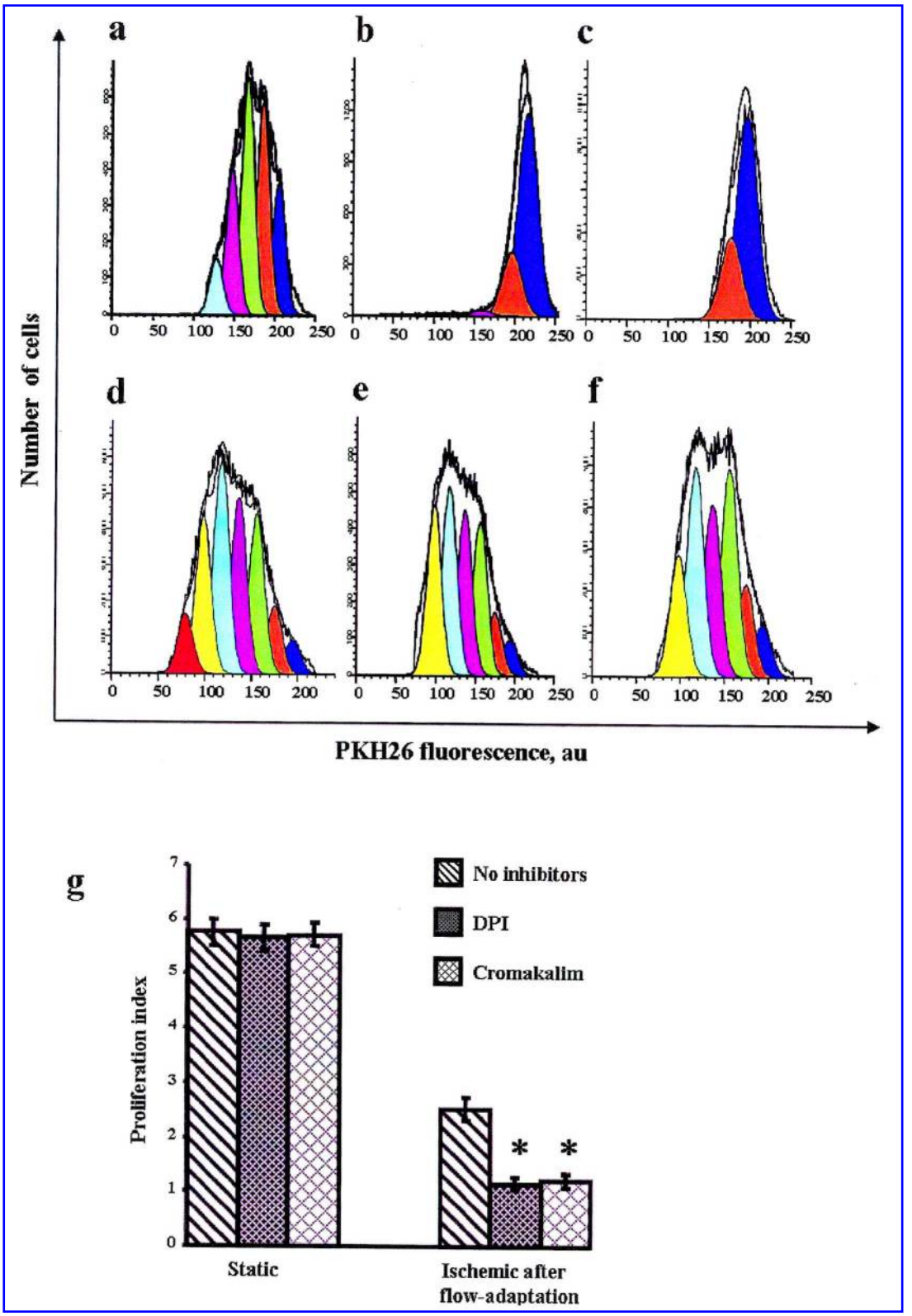

FIG. 8. The effect of inhibitors of ROS generation on proliferation of RPMVEC. Cell proliferation was determined by PKH26 fluorescence intensity of CD31-FITC-positive cells using ModFit software. Proliferation was determined in subconfluent static culture for 96 h and in response to 24 h of ischemia after flow adaptation for 72 h at 5 dynes/cm^2. Experiments were performed in the presence or absence of DPI (10 μM) or cromakalim (30 μM). (**a**) Flow-adapted RPMVEC subjected to ischemia, no inhibitors. (**b**) Flow-adapted cells followed by ischemia in the presence of DPI. (**c**) Flow-adapted cells followed by ischemia in the presence of cromakalim. (**d**) Static subconfluent cells, no inhibitors. (**e**) Static subconfluent cells in the presence of DPI. (**f**) Static subconfluent cells in the presence of cromakalim. (**g**) Means ± SE ($n = 5$ for static subconfluent and $n = 3$ for all other conditions). *$p < 0.05$ for ischemia with either inhibitor vs. ischemia alone. au, arbitrary units.

ent cells (Fig. 8e–g) in contrast to their effects on flow-adapted ischemic cells.

DISCUSSION

The isolated lung model used in our laboratory has provided extensive evidence that production of ROS occurs during the ischemic period in the ventilated lung (3–5, 27). We have postulated that the removal of the mechanical stimulus as a result of decreased perfusate flow (ischemia) initiates oxidant generation by EC through activation of the NADPH oxidase pathway and that ROS generation leads to EC proliferation (12, 13). We have further suggested that the primary event is endothelial plasma membrane depolarization due to closure of shear-activated K_{ATP} channels (9); indeed, EC membrane depolarization associated with high extracellular K^+ also results in ROS generation (2).

We further evaluated ischemia-induced ROS generation with several *in vitro* models. BPAEC were grown and flow-adapted in an artificial capillary system (26, 27). To simulate oxygenated ischemia as experienced by EC in the air-ventilated lung, we interrupted perfusate flow over the luminal surface of the cells leading to an abrupt reduction in shear stress while oxygenation of cells was provided through the porous capillaries by medium flow through the abluminal ports. As a second model, BPAEC or RPMVEC were flow-adapted in a parallel plate chamber (9, 19). To measure ROS, we used H_2DCF diacetate, a nonfluorescent probe that is deacetylated intracellularly and can be converted by oxidants to the fluorescent product DCF (5, 8, 21). With interruption of shear stress, EC that had been flow-adapted showed a significant increase in DCF-positive cells, indicating oxidation of the fluorophore H_2DCF (19, 26). ROS generation with ischemia in both lung and cell models was blocked by the presence of DPI, a flavoprotein inhibitor that inhibits NADPH oxidase (4, 19, 26). Cromakalim, a K_{ATP} channel agonist that inhibits EC membrane depolarization with ischemia (9, 22), also inhibited ROS generation (5). The present study using RPMVEC cultured in the artificial capillary system confirms previous observations with BPAEC that this model simulates the behavior of lung EC *in situ* with respect to oxidant generation in ischemia.

The major goal of the present study was to evaluate the cell proliferative response associated with ischemia-induced ROS generation. To quantitate the proliferation of cells in flow cytometry, fluorescent dyes were used to stain cytoplasm or lipid bilayer of the plasma membrane. Long-chain aliphatic dyes such as PKH26 become integrated into the lipid matrix of the membrane and appear to remain in the cell with considerable stability (16). The amount of dye in a cell is then partitioned equally between daughter cells during mitosis and therefore decreases by half at each cell division. If the characteristics of the logarithmic amplifier on a flow cytometer are known (*e.g.,* 3 or 4 log decades full scale), then the software deconvolution algorithms can derive, from a higher histogram of fluorescence intensity, the proportion of cells that undergo a particular number of divisions (6). In addition, if lineage-specific antibodies are used in a multicolor protocol, it is possible to phenotype the cells that proliferate (6, 16). We have applied the fluorescence dye method and deconvolution software to quantitate the precursor frequencies of a subpopulation of proliferating cells defined as endothelial by CD31-FITC positivity. We used PKH26 because of the potential of EC for asymmetrical cell division (tetraploid and aneuploid), in addition to the diploid population that was used for cell-cycle analysis.

This study confirms our previous results (26) that flow-adapted EC *in vitro* proliferate in response to simulated ischemia. The cell proliferative response depended on the duration of flow adaptation; at 5 dynes/cm^2, 60–72 h of adaptation to flow was necessary for maximal response to subsequent ischemia. Therefore, the mechanism for priming this response to altered flow presumably requires increased expression of cellular mechanoresponsive elements. We have demonstrated a significant induction of K_{ATP} channels during the flow adaptation period and have postulated that these channels can initiate cell signaling events associated with loss of shear (9). It is likely that other key proteins also play a role in the flow-adaptive events that are subsequently associated with the response to ischemia.

We investigated the possible role of cellular apoptosis in the initiation of ischemia-mediated cellular proliferation. Cell death with ischemia in the present experiments seems unlikely because there was no difference in TUNEL and annexin V binding assays between control and ischemic cells, and apoptotic cells comprised only 5% of the cell population. Further, the yield of cells from the cartridges following trypsinization was greater for ischemia compared with continued flow experiments. Thus, proliferation with ischemia did not appear to be a response to cell death.

Our previous studies indicated that lung EC *in situ* exhibit plasma membrane depolarization during ischemia, which results in ROS generation via activation of NADPH oxidase (3, 4, 22). Generation of ROS with ischemia *in vitro* was associated with activation of NF-κB and AP-1 and increased DNA synthesis (26). Further, ROS can mediate Ras-induced cell-cycle progression and mammalian cell proliferation (17, 20). The present *in vitro* study confirms ROS generation with ischemia and shows that its inhibition by relatively nontoxic agents (cromakalim and DPI) that exert their effect by different mechanisms prevents cellular proliferation. Thus, cell proliferation with this ischemia model appears to result from signals associated with ROS. An alternative explanation for the results is that depletion of cells from the capillaries by mechanical stress associated with flow results in an absence of "contact inhibition," so that cell division resumes when the antiproliferative effect of shear stress is discontinued. This possibility is excluded by the lack of effect of cromakalim and DPI on subconfluent cells grown under static conditions. Therefore, the mechanism for initiation of cell division appears to be different for ischemia after flow adaptation versus subconfluent static cell cultures. For the more physiological flow-adapted state, cell division with ischemia is a response to cell signaling via ROS.

Exposure of EC to steady laminar flow has been shown previously to decrease cellular proliferation (1, 17) and is confirmed in the present study. Accumulation of cells in the G0/G1 phase after exposure to shear stress accompanied by a decrease in the number of cells in the S and G2/M phases indicates that steady laminar shear stress blocks a cell-cycle event that occurs before entry into the S phase. Flow cessation with flow-adapted cells results in the inverse effect, namely, cellu-

lar proliferation (26). Thus, shear stress appears to play a key regulatory role in maintenance of the EC population. Derangement of blood flow (such as at branch orifices) may release cells from shear stress-mediated inhibition and induce cell proliferation, thereby disturbing the stability of the EC monolayer (25).

In summary, we have shown using an *in vitro* model of oxygenated "ischemia" that flow-adapted EC respond to cessation of flow with increased ROS production and cellular proliferation. Proliferation in this model is not a response to cell death. We postulate that ROS stimulate proliferation through a signaling cascade is a response to the altered shear stress in an effort at neovascularization.

ACKNOWLEDGMENTS

This work was supported by NIH grant HL60290. We thank Drs. Sheldon Feinstein and Zhihua Wei for helpful suggestions, Mrs. Kathy Notarfrancesco, Mr. Andrew Bantly, and Dr. Irina Kotelnikova for excellent technical support, and Jennifer Rossi for typing the manuscript. Results of this study were presented in preliminary form at the Experimental Biology meeting in San Diego, CA, April 2003.

ABBREVIATIONS

AP-1, activator protein-1; BPAEC, bovine pulmonary artery endothelial cells; DCF, dichlorofluorescein; DMEM, Dulbecco's modified Eagle's medium; DPI, diphenyleneiodonium chloride; EC, endothelial cells; FACS, fluorescence-activated cell sorter; FBS, fetal bovine serum; FITC, fluorescein isothiocyanate; H_2DCF, 2′,7′-dichlorodihydrofluorescein; NF-κB, nuclear factor-κB; PBS, phosphate-buffered saline; PCNA, proliferating cell nuclear antigen; ROS, reactive oxygen species; RPMVEC, rat pulmonary microvascular endothelial cells; TNFα, tumor necrosis factor-α; TUNEL, terminal dUTP nucleotide end labeling.

REFERENCES

1. Akimoto S, Mitsumata M, Sasaguri T, and Yoshida Y. Laminar shear stress inhibits vascular endothelial cell proliferation by inducing cyclin-dependent kinase inhibitor p21(Sdi1/Cip1/Waf1). *Circ Res* 86**:** 185–190, 2000.
2. Al-Mehdi AB, Shuman H, and Fisher AB. Oxidant generation with K^+-induced depolarization in the isolated perfused lung. *Free Radic Biol Med* 23: 47–56, 1997.
3. Al-Mehdi AB, Shuman H, and Fisher AB. Intracellular generation of reactive oxygen species during nonhypoxic lung ischemia. *Am J Physiol* 272: L294–L300, 1997.
4. Al-Mehdi AB, Zhao G, Dodia C, Tozawa K, Costa K, Muzykantov V, Ross C, Blecha F, Dinauer M, and Fisher AB. Endothelial NADPH oxidase as the source of oxidants in lungs exposed to ischemia or high K^+. *Circ Res* 83: 730–737, 1998.
5. Al-Mehdi AB, Zhao G, Tozawa K, and Fisher AB. Depolarization-associated iron release with abrupt reduction in pulmonary endothelial shear stress *in situ*. *Antioxid Redox Signal* 2: 335–345, 2000.
6. Bagwell CB and Adams EG. Fluorescence spectral overlap compensation for any number of flow cytometry parameters. *Ann N Y Acad Sci* 677: 167–184, 1993.
7. Bartling B, Tostlebe H, Darmer D, Holtz J, Silber RE, and Morawietz H. Shear stress-dependent expression of apoptosis-regulating genes in endothelial cells. *Biochem Biophys Res Commun* 278: 740–746, 2000.
8. Carter WO, Narayanan PK, and Robinson JP. Intracellular hydrogen peroxide and superoxide anion detection in endothelial cells. *J Leukoc Biol* 55: 253–258, 1994.
9. Chatterjee S, Al-Mehdi A-B, Levitan I, Stevens T, and Fisher AB. Shear stress increases expression of a K_{ATP} channel in rat and bovine pulmonary vascular endothelial cells. *Am J Physiol Cell Physiol* 285: C959–C967, 2003.
10. Dimmeler S, Hermann C, Galle J, and Zeiher AM. Upregulation of superoxide dismutase and nitric oxide synthase mediates the apoptosis-suppressive effects of shear stress on endothelial cells. *Arterioscler Thromb Vasc Biol* 19: 656–664, 1999.
11. Douglas RS, Pletcher CH Jr, Nowell PC, and Moore JS. Novel approach for simultaneous evaluation of cell phenotype, apoptosis, and cell cycle using multiparameter flow cytometry. *Cytometry* 32: 57–65, 1998.
12. Fisher AB, Al-Mehdi AB, and Manevich Y. Shear stress and endothelial cell activation. *Crit Care Med* 30: S192–S197, 2002.
13. Fisher AB, Al-Mehdi AB, Wei Z, Song C, and Manevich Y. Lung ischemia: endothelial cell signaling by reactive oxygen species. *Adv Exp Med Biol* 510: 343–347, 2003.
14. Givan AL, Fisher JL, Waugh M, Ernstoff MS, and Wallace PK. A flow cytometric method to estimate the precursor frequencies of cells proliferating in response to specific antigens. *J Immunol Methods* 230: 99–112, 1999.
15. Haendeler J, Zeiher AM, and Dimmeler S. Nitric oxide and apoptosis. *Vitam Horm* 57: 49–77, 1999.
16. Horan PK and Slezak SE. Stable cell membrane labeling. *Nature* 340: 167–168, 1989.
17. Irani K, Xia Y, Zweier JL, Sollott SJ, Der CJ, Fearon ER, Sundaresan M, Finkel T, and Goldschmidt-Clermont PJ. Mitogenic signaling mediated by oxidants in Ras-transformed fibroblasts. *Science* 275: 1649–1652, 1997.
18. Lounsbury KM, Stern M, Taatjes D, Jaken S, and Mossman BT. Increased localization and substrate activation of protein kinase C delta in lung epithelial cells following exposure to asbestos. *Am J Pathol* 160: 1991–2000, 2002.
19. Manevich Y, Al-Mehdi A, Muzykantov V, and Fisher AB. Oxidative burst and NO generation as initial response to ischemia in flow adapted endothelial cells. *Am J Physiol Heart Circ Physiol* 280: H2126–H2135, 2001.
20. Moore KA, Sethi R, Doanes AM, Johnson TM, Pracyk JB, Kirby M, Irani K, Goldschmidt-Clermont PJ, and Finkel T. Rac1 is required for cell proliferation and G2/M progression. *Biochem J* 326 (Pt 1): 17–20, 1997.
21. Royall JA and Ischiropoulos H. Evaluation of 2′,7′-dichlorofluorescin and dihydrorhodamine 123 as fluorescent probes for intracellular H_2O_2 in cultured endothelial cells. *Arch Biochem Biophys* 302: 348–355, 1993.
22. Song C, Al-Mehdi AB, and Fisher AB. An immediate endothelial cell signaling response to lung ischemia. *Am J Physiol*

Lung Cell Mol Physiol 281: L993–L1000. Corrigenda in: *Am J Physiol Lung Cell Mol Physiol* 282: section L following table of contents, 2002.
23. Song HK, Noorchashm H, Lieu YK, Rostami S, Greeley SA, Barker CF, and Naji A. Tracking alloreactive cell division in vivo. *Transplantation* 68: 297–299, 1999.
24. Stevens T, Creighton J, and Thompson WJ. Control of cAMP in lung endothelial cell phenotypes. Implications for control of barrier function. *Am J Physiol* 277: L119–L126, 1999.
25. Tricot O, Mallat Z, Heymes C, Belmin J, Leseche G, and Tedgui A. Relation between endothelial cell apoptosis and blood flow direction in human atherosclerotic plaques. *Circulation* 101: 2450–2453, 2000.
26. Wei Z, Costa K, Al-Mehdi AB, Dodia C, Muzykantov V, and Fisher AB. Simulated ischemia in flow adapted endothelial cells leads to generation of reactive oxygen species and cell signaling. *Circ Res* 85: 682–689, 1999.
27. Wei Z, Al-Mehdi AB, and Fisher AB. Signaling pathway for nitric oxide generation with simulated ischemia in flow adapted endothelial cells. *Am J Physiol Heart Circ Physiol* 281: H2226–H2232, 2001.

Address reprint requests to:
Aron B. Fisher, M.D.
Institute for Environmental Medicine
University of Pennsylvania Medical Center
One John Morgan Building
Philadelphia, PA 19104–6068

E-mail: abf@mail.med.upenn.edu

Received for publication October 23, 2003; accepted November 10, 2003.

This article has been cited by:

1. Aron B. Fisher. 2011. Oxidant Stress in Pulmonary Endothelia. *Annual Review of Physiology* **74**:1, 110301101907077. [CrossRef]
2. Eirini Kefaloyianni, William A. Coetzee. 2011. Transcriptional Remodeling of Ion Channel Subunits by Flow Adaptation in Human Coronary Artery Endothelial Cells. *Journal of Vascular Research* **48**:4, 357-367. [CrossRef]
3. Shampa Chatterjee , Aron B. Fisher Detection of Reactive Oxygen Species (ROS) with Altered Shear Stress in the Lung Endothelium 213-216. [Abstract] [Summary] [Full Text PDF] [Full Text PDF with Links]
4. Shampa Chatterjee, Kenneth E. Chapman, Aron B. Fisher. 2008. Lung Ischemia: A Model for Endothelial Mechanotransduction. *Cell Biochemistry and Biophysics* **52**:3, 125-138. [CrossRef]
5. Tatyana Milovanova, Shampa Chatterjee, Brian J. Hawkins, NanKang Hong, Elena M. Sorokina, Kris DeBolt, Jonni S. Moore, Muniswamy Madesh, Aron B. Fisher. 2008. Caveolae are an essential component of the pathway for endothelial cell signaling associated with abrupt reduction of shear stress. *Biochimica et Biophysica Acta (BBA) - Molecular Cell Research* **1783**:10, 1866-1875. [CrossRef]
6. Nick M. Matharu, Helen M. McGettrick, Mike Salmon, Steve Kissane, Rajiv K. Vohra, G.Ed. Rainger, Gerard B. Nash. 2008. Inflammatory responses of endothelial cells experiencing reduction in flow after conditioning by shear stress. *Journal of Cellular Physiology* **216**:3, 732-741. [CrossRef]
7. J VANEPPS, D VORP. 2007. Mechanopathobiology of Atherogenesis: A Review. *Journal of Surgical Research* **142**:1, 202-217. [CrossRef]
8. Alison C. Cave , Alison C. Brewer , Anilkumar Narayanapanicker , Robin Ray , David J. Grieve , Simon Walker , Professor Ajay M. Shah . 2006. NADPH Oxidases in Cardiovascular Health and Disease. *Antioxidants & Redox Signaling* **8**:5-6, 691-728. [Abstract] [Full Text PDF] [Full Text PDF with Links]
9. Valerian E. Kagan , Peter J. Quinn . 2004. Toward Oxidative Lipidomics of Cell Signaling. *Antioxidants & Redox Signaling* **6**:2, 199-202. [Abstract] [Full Text PDF] [Full Text PDF with Links]
10. Dipak K. Das Methods in Redox Signaling . [Citation] [Full Text HTML] [Full Text PDF] [Full Text PDF with Links]